Available online at www.sciencedirect.com

ScienceDirect

MATTER AND RADIATION AT EXTREMES

Matter and Radiation at Extremes 1 (2016) 192—200

www.journals.elsevier.com/matter-and-radiation-at-extremes

Review article

A general comparison between tokamak and stellarator plasmas

Yuhong Xu*

Southwestern Institute of Physics, PO Box 432, Chengdu 610041, People's Republic of China

Received 31 March 2016; revised 5 June 2016; accepted 8 June 2016
Available online 12 July 2016

Abstract

This paper generally compares the essential features between tokamaks and stellarators, based on previous review work individually made by authors on several specific topics, such as theories, bulk plasma transport and edge divertor physics, along with some recent results. It aims at summarizing the main results and conclusions with regard to the advantages and disadvantages in these two types of magnetic fusion devices. The comparison includes basic magnetic configurations, magnetohydrodynamic (MHD) instabilities, operational limits and disruptions, neoclassical and turbulent transport, confinement scaling and isotopic effects, plasma rotation, and edge and divertor physics. Finally, a concept of quasi-symmetric stellarators is briefly referred along with a comparison of future application for fusion reactors.

PACS codes: 52.55.Fa; 52.55.Hc; 52.30.Cv; 52.25.Fi; 52.55.-s; 52.55.Rk

Keywords: Tokamaks; Stellarators; Magnetohydrodynamic (MHD); Plasma transport and confinement; Divertor

1. Introduction

In the study of controlled nuclear fusion for producing useful amounts of energy, the most advanced candidates to realize the fusion reaction by magnetically confining thermonuclear plasmas are *tokamaks* and *stellarators*. Over the last 60 years, fusion research has been intensely performed in tokamaks in various laboratories across the world and its remarkable progress leads to an initiation of the ITER project, which is the world's largest tokamak to be designed and operated as the first fusion test reactor of burning deuterium-tritium plasmas [1]. In parallel, the fusion programme in stellarators has also made significant achievements, although less effort was made for the stellarator devices due to the technical complexity in comparison with tokamaks. The physical properties of stellarators are therefore less understood than they deserve to be. In fact, a lot of key concepts in magnetic confinement physics stemmed from stellarators [2]. The recently successful operation of the Wendelstein 7-X in Germany [3] further indicates that great strides have been taken toward the development of a fusion reactor in the stellarator as an alternative model of a power plant.

For *tokamaks* and *stellarators*, both of their concepts have innate advantages and disadvantages with regard to technical and physical aspects of a fusion device on the way to burning plasmas. In this paper, a general comparison of the magnetic configuration, magnetohydrodynamic (MHD) instabilities and operational limits, neoclassical and turbulent transport, plasma confinement, plasmas rotation and edge physics is briefly reviewed on the similarities and differences between the tokamak and stellarator plasmas.

2. Magnetic configurations

For a toroidal plasma confinement system, the plasmas are confined by a magnetic field. In order to have an equilibrium between the plasma pressure and the magnetic forces it is

* Corresponding author.
E-mail address: xuyh@swip.ac.cn.
Peer review under responsibility of Science and Technology Information Center, China Academy of Engineering Physics.

http://dx.doi.org/10.1016/j.mre.2016.07.001

necessary to have a rotational transform of the toroidal magnetic field. Such a rotational transform may prevent the curvature drift of the guiding center of plasma particles towards the wall. As proposed by Spitzer and Mercier [4,5], there are three different ways to twist the magnetic field: (i) creating a poloidal field by a toroidal electric current; (ii) rotating the poloidal cross-section of stretched flux surfaces around the torus; (iii) making the magnetic axis non-planar. While tokamaks use the first approach, stellarators usually rely on the latter two methods, namely, in tokamaks the twisting is produced by a toroidal plasma current and in stellarators by external non-axisymmetric coils. These two types of configuration are depicted in Fig. 1. This brings clear difference for the two systems. For example, tokamaks are axisymmetric and can confine all collisionless particles and have relatively good plasma confinement. But the toroidal current is normally generated by a transformer, which makes the device vulnerable to current-driven instabilities and difficult to operate in a steady state. The stellarators, on the other hand, are inherently current free, and thus, able to operate the plasma in a steady state. But more unconfined particle orbits in stellarators can lead to high neoclassical transport of energetic and thermal particles.

The geometrical parameters also differ much for tokamaks and stellarators. In tokamaks the aspect ratio R/a (R and a represent the major and minor radii, respectively) is usually in a range of 2.5–4, and the value is even smaller for spherical tokamaks. In stellarators, to avoid resonances between the field lines and harmonics of the symmetry of the configuration, the device is designed to have small rotational transforms per period, which results in much larger aspect ratios ($R/a = 5-12$) in the present-day stellarators [6]. As a consequence, the effective plasma volume in tokamaks is much larger than in stellarators.

The profiles of the safety factor (q) and magnetic shear ($s = r\partial q/q\partial r$) are also very different between the two systems. Tokamaks normally operate with positive magnetic shear throughout the entire plasmas whereas in stellarators the shear is negative (except for non-planar types, which may have a zero magnetic shear). A further difference lies in the shape of the plasma cross-section. In tokamaks the plasma cross-section is toroidally symmetric, while in a three-dimensional stellarator the shape varies as a function of the toroidal angle, as illustrated in Fig. 1.

3. MHD instabilities, operational limits and disruptions

In fusion plasmas, the MHD instability plays a crucial role in determining the achievable plasma parameters, advanced scenarios and operational limits. Theoretically, for various classes of MHD activities, such as sawtooth oscillations, kink instabilities, resistive and neoclassical tearing modes, the basic destabilizing forces arise from current and pressure gradients together with adverse magnetic field curvatures [7]. The beta limit and density limit are also treated as two key elements that govern the basic design and plasma performance in reactor devices. As eventual consequences of the MHD instability, the occurrence of plasma disruptions will determine the operational lifetime of machine components, especially those associated with plasma particle and energy exhaust.

In tokamaks, the existence of toroidal plasma current leads to macroscopic and microscopic effects of the MHD instability, which set constraint on the operational feasibility. Therefore, active control of MHD instabilities becomes a serious issue for reactor tokamaks. In contrast, for stellarators the avoidance of the toroidal plasma current brings great advantages. The MHD instabilities are usually absent due to no or little net plasma current. Of course, in stellarators two small plasma current components also exist [8]. One is the bootstrap current driven by pressure gradients in the banana regime at low collisionality, which is similar to tokamaks. The other is the parallel Pfirsch–Schluter current used to compensate the non-zero poloidal plasma current, which appears to force balance the radial pressure gradient, so that the total plasma current is divergence-free ($\nabla \cdot \boldsymbol{J} = 0$). But both sorts of current are substantially small to destabilize big MHD modes.

In tokamaks the neoclassical tearing mode (NTM) can be excited by the perturbation of a bootstrap current, which is proportional to the pressure gradient [7]. When a seed island forms, the local pressure gradient within the magnetic island is reduced by the transport parallel to the flux tube of field lines, which results in a reduction of the bootstrap current. In tokamaks such a negative current perturbation causes further growing of the island [7]. However, in stellarators, because the global magnetic shear is opposite to that in tokamaks, the reduction of the bootstrap current within a seed island makes the island shrink rather than grow [9–11]. Thus, the plasma

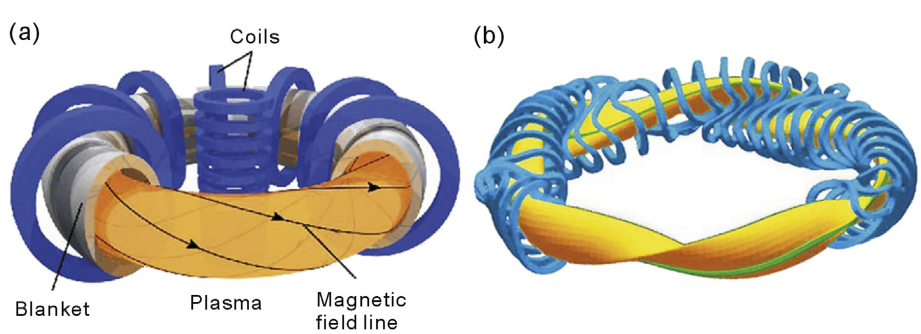

Fig. 1. Schematics of magnetically confined plasmas in (a) tokamaks; (b) stellarator configurations. In the tokamak, the rotational transform of a helical magnetic field is formed by a toroidal field generated by external coils together with a poloidal field generated by the plasma current. In the stellarator, the twisting field is produced entirely by external non-axisymmetric coils.

pressure in stellarators often has a function to heal magnetic islands.

The beta limit arises from unstable MHD modes driven by plasma pressure gradients, resulting in the attainable ratio of plasma thermal pressure to magnetic field pressure ($\beta = P/(B^2/2\mu_0)$) limited by a critical value [12]. The tokamak beta limit is usually related to the ideal-MHD ballooning mode, and hence, increases with plasma current and decreases with the strength of magnetic field [13]. However, in stellarators this beta limit appears to be soft, far beyond the ideal ballooning limit. Because energetic ions show stabilizing impact on ballooning modes in stellarators, a significant fraction of the plasma pressure has been obtained there (volume-averaged $<\beta>$ reaches 5%) [14]. In Large Helical Device (LHD), a distinct central beta limit has been observed in super high-density plasmas accompanied by an internal diffusion barrier, for which a very peaked pressure profile is generated and the Shafranov shift grows over half of the minor radius [15]. Although it is not entirely clear for high obtainable β value in stellarators, the effects of finite Larmor radius seem to play an important role.

In fusion plasmas, the maximum achievable density is limited basically due to the increase of impurity radiation with increasing density, which eventually leads to a collapse [16,17]. In tokamaks, the radiative collapse may cause a rapid cooling of the outer plasma boundary and a contraction of the current profile, producing a strong MHD instability around $q = 2$ magnetic surface and consequently a dramatic disruption, which usually follows the “Greenwald” limit scaling [18]. Another specific edge phenomenon observed in tokamaks to restrain the plasma density is multifaceted asymmetric radiation from the edge (MARFE), a zone of high radiation located on the inner side of the torus [19,20]. The MARFE is thought to be the result of a radiation-driven thermal instability, i.e., the plasma is cooled by radiation emission and the cooling itself results in increased radiation being emitted and hence further cooled down. In stellarators, because of the absence of toroidal current, the “Greenwald” limit does not exist, but instead, the density is limited by the absorbed power along with magnetic field and plasma volume [21,22]. As such, the stellarators often operate at a higher density than tokamaks do. In the LHD, a super-dense core plasma ($>1 \times 10^{21}$ m^{-3}) has been attained [23].

Owing to various MHD instabilities, a major disruption may happen in tokamaks followed by a complete loss of the plasma current. Disruptions pose serious problems for tokamak development as they firstly limit the range of operation in current and density, and secondly lead to large mechanical stresses and intense heat loads to the plasma facing components of reactor devices. In fact, strategies for disruption prediction and mitigation are urgently needed for ITER [1]. In contrast, stellarators do not experience terminating disruptions except for using transformers to excite toroidal current and hence tearing modes [24]. So far, the LHD has not yet suffered a dramatic disruption after 1,20,000 discharges [23].

In fusion plasmas, the energetic particles induced mainly by injected neutrals and ions accelerated by radio-frequency-wave heating, may also drive MHD modes, such as fishbones and Alfven eigenmodes (AEs). As the fast particle pressure is proportional to the slowing-down time, which decreases with increasing plasma density, the Alfvenic modes are expected to be weaker in instellarators than in tokamaks since high density can be reached in stellarators. For toroidicity-induced shear AEs they arise in the gaps of the continuous Alfvenic spectrum [7]. The axisymmetry breaking in stellarators leads to additional gaps so that more wave-particle resonances and more types of toroidal AEs may appear in stellarators than in tokamak [25].

4. Transport

4.1. Neoclassical transport

In toroidal devices, the magnetic field is inhomogeneous, i.e., stronger at the inner side of the torus than at the outer side. The curvature and gradient of the magnetic field result in extra forces and drifts that are not present in cylindrical configurations. The collisional transport related to this inhomogeneous, curved field is called neoclassical transport [26]. The theoretical groundwork for neoclassical transport has been well established in the 1970s for axisymmetric toroidal plasmas [27,28]. For tokamaks, the neoclassical random-walk step size is usually limited by the banana width (the radial width of the guiding center orbit of a trapped particle on the outer side of the torus), and hence, the transport is always local if the width is smaller than the scale length of the local gradient. However, for stellarators, in the case of low collisionality the step size can be very large due to the influence of the helical magnetic ripple. This may break the localization of the transport [29,30]. In tokamaks, the variation of transport diffusivity with collision frequency (ν) is normally divided into three regimes: the banana regime with low ν, the Pfirsch−Schluter regime with high ν and a plateau in between [7]. For both electrons and ions, the diffusion coefficient increases with ν in the banana and Pfirsch−Schluter regimes. In stellarators, there exist more regimes in low collisionality cases, which are scaled as $\nu^{0.5}$ and $1/\nu$. Moreover, the electrons and ions are often in different regimes, and the larger diffusivity of ions than electrons often violates the ambipolarity [29,30]. For electrons they usually lie in the $1/\nu$ regime. At low collisionality of $\nu^{0.5}$ and $1/\nu$ regimes, the diffusion coefficient in stellarators is much larger than in tokamaks (see Fig. 2) [31]. Therefore, in stellarators the neoclassical transport losses are expected to dominate at high electron temperature, which is apparently a disadvantage to be overcome for stellarators.

4.2. Turbulence and turbulent transport

The theoretical picture of turbulent transport is that the free energy, such as temperature or density gradient, drives micro-scale drift-type instabilities and a steady level of fluctuations, which lead to a radial transport of particles and energy. For tokamak plasmas this turbulence-induced transport is thought to be responsible for the observed anomalous transport, in

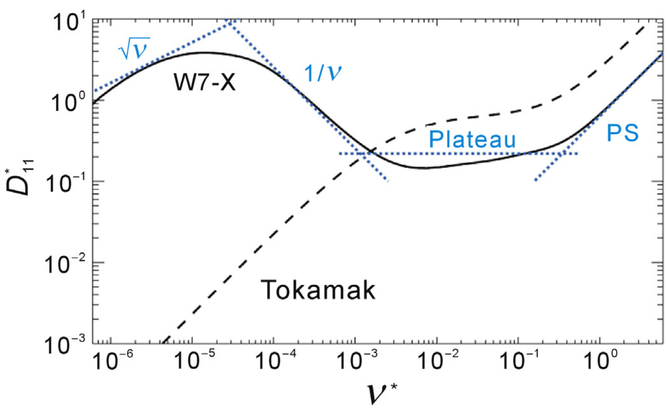

Fig. 2. Comparison of diffusion coefficient versus collisionality between tokamaks (dotted curve) and the W7-X stellarator (solid curve) in different regimes [31].

particular, the electron thermal transport which is up to two orders of magnitude higher than theoretical predictions [1,7]. For stellarators, although the neoclassical transport is much higher than in tokamak at high temperature in the plasma core, the turbulent transport also plays an important role in the cooler parts, where the $\nu^{0.5}$ and $1/\nu$ regimes do not work [8]. For the collisionless instabilities with electrostatic approximation, the dispersion relation of the curvature-driven ion-temperature-gradient (ITG) mode appears to be the same to both tokamaks and stellarators [32,33]. Whereas in tokamaks the trapped-electron mode (TEM), driven by the density gradient, routinely results in outward transport flux, the TEM is stabilized in stellarators within the usual drift-wave ordering $k_{//}V_{\mathrm{Te}} >> \omega$ [34,35]. Gyrokinetic simulations (*e.g.*, EUTERPE, FULL, GENE, GS2, GKV codes [36–40]) indicate that, unlike the typical situation in tokamaks, there is no sign of rapidly growing kinetic ballooning modes at high plasma pressure $<\beta>$. It seems that stellarators benefit from their large local magnetic shear as well as the negative global magnetic shear, which tends to stabilize curvature-driven modes [41–43]. In many tokamaks the locally reversed negative shear has also been observed accompanied with improved confinement and a strong pressure gradient [44–47]. Because the strong pressure gradient may induce a large bootstrap current which is favorable to form the reversed q profile and negative magnetic shear, it in turn has a stabilizing effect on ballooning modes. For the concept of the advanced tokamak operation scenario, realization of reversed magnetic shear with a large bootstrap current has been proposed as a key approach [48]. However, on the other hand, in stellarators the zonal-flows (electric field fluctuations being symmetric on magnetic flux surface ($m = n = 0$) with finite radial wavenumbers) suffer stronger damping than tokamaks through electron collisions due to non-ambipolar neoclassical transport.

Experimentally, for investigating mechanisms of turbulent transport, the turbulence amplitudes in density, temperature, potential, magnetic fluctuations and associated transport have been measured in many fusion devices and some comparisons were also made among several tokamaks and stellarators [6]. In the TEXT tokamak and ATF stellarator, the results of edge turbulence showed an overall similarity [49]. In the TJ-IU tokamak and TJ-I stellarator, the turbulence-induced particle flux exhibited similar intermittent behavior along with non-Gaussian distribution [50]. In the scrape-off-layers of ASDEX tokamak and W7-AS stellarator, the turbulence structures of density fluctuations both propagate poloidally in the ion-diamagnetic drift direction [51]. Moreover, a concurrent increase of density fluctuation magnitudes and the electron diffusivity towards the plasma edge were observed in the TFTR tokamak and the W7-AS stellarator [52,53]. In the bulk plasma region, reductions of the density fluctuation level with increasing plasma density were also observed in the Tore Supra tokamak and W7-AS stellarator (see Fig. 3), and in both devices the density fluctuations correlate with the electron thermal diffusivity [54,55].

4.3. Energy confinement and isotope effects

To obtain thermonuclear conditions in fusion devices, it is necessary to confine the plasma for a sufficient time. Being different from the plasma discharge duration, the energy confinement time (τ_{E}) is defined as the plasma stored energy W divided by the absorbed heating power (P) subtracted for the variation of the plasma energy, i.e., $\tau_{\mathrm{E}} = W/(P - \mathrm{d}W/\mathrm{d}t)$. As one of the key fusion-relevant parameters, the value of τ_{E} has been measured in both tokamaks and stellarators. The plasma confinement behavior can be conventionally classified into four categories [7]: (i) Ohmically heated plasmas; (ii) low-mode (L-mode, where the confinement degrades with increased heating power); (iii) high mode (H-mode, where the confinement improves abruptly when sufficient power is applied) and (iv) enhanced confinement with internal transport barrier (ITB) and reversed magnetic shear. Hitherto, the physical understanding of these different confinement behaviors is still lacking. As a consequence, it is necessary to resort to empirical scaling expressions for the confinement time in various regimes. For tokamaks, the ITER 89-P scaling $\tau_{\mathrm{E,\,ITER89\text{-}P}} = 0.048\, M^{0.5}\, I^{0.85}\, n^{0.1}\, B^{0.2}\, \kappa^{0.5}\, R^{1.2}\, a^{0.3}\, P^{-0.5}$ [56] and the IPB98(y, 2) scaling $\tau_{\mathrm{E,\,IPB98}(y,\,2)} = 0.145\, M^{0.19}\, I^{0.93}\, n^{0.41}\, B^{0.2}\, \kappa^{0.78}\, R^{1.39}\, a^{0.58}\, P^{-0.69}$ [57] have been obtained from the L-mode and ELMy H-mode database, respectively. Here the M, I, n, B, κ, R, a and P denote the atomic mass, plasma current, line-averaged density, toroidal magnetic field, plasma enlongation, major plasma radius, minor plasma adius and the total heating power, respectively. For stellarators, a common scaling for the stellarator L-mode confinement is given by the ISS95 expression $\tau_{\mathrm{E,\,ISS95}} = 0.79\, a^{2.21}\, R^{0.65}\, n^{0.51}\, B^{0.83} P^{-0.59} \iota^{0.4}$, where ι is the rotational transform [58]. Considering the dependence on the plasma current and other geometrical parameters, the scaling expressions for tokamaks and stellarators are obviously different. However, if we replace plasma current in tokamak expression by the magnetic field and the safety factor q ($q = 2\pi/\iota$), the scaling expressions in tokamaks and stellarators become comparable. Detailed discussion on this aspect has been given in Ref. [6]. A

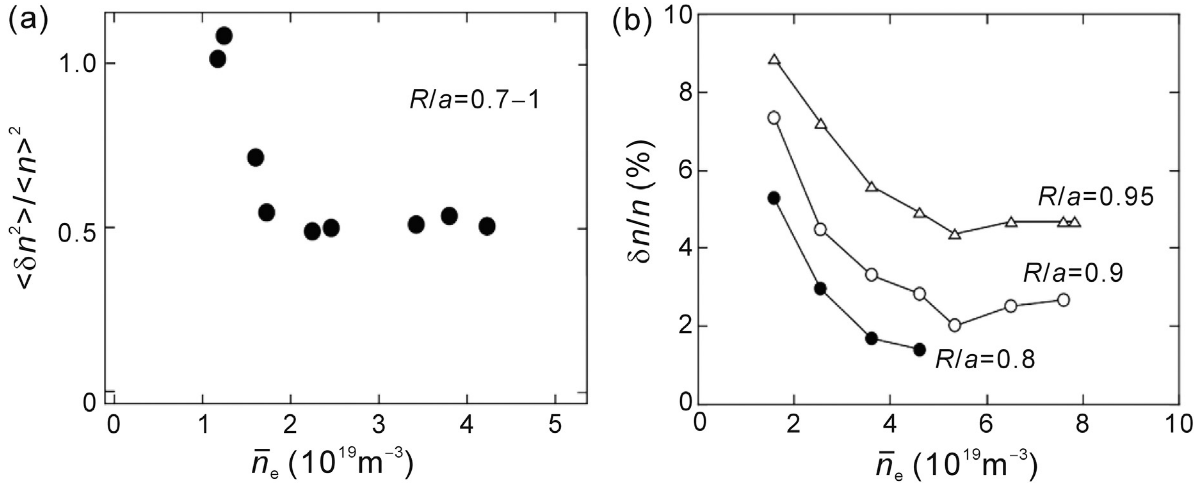

Fig. 3. Variation of density fluctuation amplitudes with increasing line-averaged density measured in (a) Tore Supra tokamak and (b) W7-AS stellarator [54].

comparison of the ISS95 scaling with experimental data from the tokamak (ITER L-mode) database and stellarator database is depicted in Fig. 4 (a), and most recently with the LHD data is shown in Fig. 4(b). The results show good consistence of the parameteric dependence.

Nevertheless, for the confinement time scaling, a clear difference emerged between tokamaks and stellarators is the isotopic effect. As seen in the above τ_E scaling expressions, for tokamaks a positive power index on the ion mass (M) indicates better confinement for heavier ions whereas for stellarators such an effect is much weaker, or even reverse in some cases [6,59]. This isotope effect gives a favorable impact on the confinement properties of fusion D-T plasmas, however, it is a counter intuitive phenomenon in the view of collisional transport model. Considering that the characteristic step size of collisional transport and turbulent structures both increase with the plasma gyroradius [60,61], increasing the mass of the isotope would imply a deleterious effect on transport. Recent experimental results of comparative studies between tokamaks and stellarators show evidence of the increase of zonal flows from hydrogen to deuterium plasmas in tokamaks while the zonal flows are damped in stellarators, suggesting possible influence of the isotopic mass on zonal flows and hence plasma confinement [61–63]. These results are consistent with theoretical predictions [40,64].

5. Plasma rotation

In the magnetically confined system, plasma rotation means the part of the fluid velocity that lies on a flux surface. The dynamic forces to drive the plasma rotation are normally the $\boldsymbol{J} \times \boldsymbol{B}$ force, externally injected neutral beam, or turbulent Reynolds stress. For tokamaks, the poloidal rotation is generally damped due to the magnetic pumping effects, which transfer the plasma kinetic energy into thermal energy, and eventually, towards the neoclassical value [65,66]. But a toroidally rotating plasma in the axisymmetric tokamaks does not suffer the magnetic pumping effect since the neoclassical transport (and the perpendicular viscosity) is usually small. Thus, in tokamaks the toroidal rotation velocity can reach a very high value, being a significant fraction of the ion thermal velocity.

In non-axisymmetric stellarators, the neoclassical transport is much larger. The plasmas follow the drift-kinetic equation model such that the fast rotation is not possible [67]. Even for a quasi-symmetric stellarator, the plasma flow turns to be impeded as well [68]. But for the homogenous $m = n = 0$ zonal flows, they have been observed in tokamaks and in stellarators as well, although for the latter the damping effect is stronger [69].

6. Edge and divertor physics

In magnetically confinement devices, the plasma is confined within closed magnetic flux surfaces and a boundary exists between plasmas and the machine-wall components. This boundary is generally called the scrape-off layer (SOL), which is determined by a solid surface (limiter) or topologically by magnetic field perturbations (divertor). Because the impurities originated from plasma-facing components (PFC) present a lot of problems, *e.g.*, the huge radiative power loss and dilution of fuel particles, reducing impurities released from the PFC and preventing them from entering the plasma core region are crucial tasks of the edge and divertor physics [7]. With the divertor configuration, plasma particles and energy leaving the confinement region are guided to the divertor target plate by open field lines. For the poloidal divertor in tokamaks, the separatrix of the SOL is formed by additional poloidal magnetic field coils, which tear up the nested flux surfaces into single or double null divertor configuration (see Fig. 5(a)–(b)). For stellarators, the divertor configuration is intrinsically developed on the base of special edge magnetic structures arising from the small radial field resonant with the rational surface [70]. Nevertheless, the stellarator divertor geometries may differ from each other, depending on the global magnetic shear. In the case of low-shear there exist

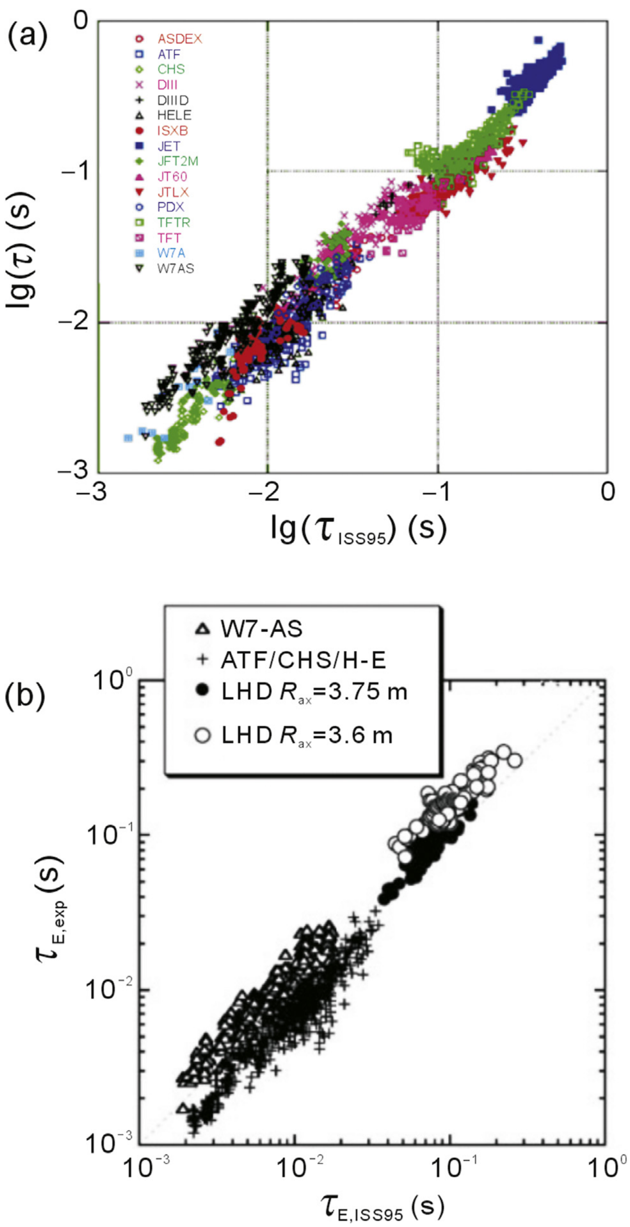

Fig. 4. (a) Comparison of the energy confinement time from the tokamak ITER L-mode database and the stellarator database with the prediction of the ISS95 scaling [58]; (b) comparison of the energy confinement time in stellarators with the prediction of the ISS95 scaling [23]. Triangles are data from the W7-AS stellarator, plus symbols are data from medium-sized heliotron/torsatron, and solid and open circles are data from LHD with two different magnetic axes.

chains of the island divertor, while in the high-shear case the divertor configuration covers many resonances which overlap and form a stochastic layer (see Fig. 5(c)−(d)) [71,72]. For tokamaks and stellarators, a significant difference in governing the divertor transport is the field-line pitch $\Theta = dx/dl_{//}$, which is typically $\Theta = 0.1$ for tokamaks and $\Theta = 0.001$ for stellarators [70]. Because of relatively large pitch angle, in tokamaks most of the heat flux across the SOL is carried by parallel heat conduction, especially for the electrons. In stellarators the small pitch makes the parallel and perpendicular transport much more comparable, even for electrons.

Experimentally, discrepancies in divertor transport have also been observed between tokamaks and stellarators. In the SOL of the ASDEX tokamak, the downstream density (n_{ed}) was measured versus the change of the plasma line-averaged density. With increasing plasma density, n_{ed} varies typically in three regimes: (i) slowly rises at the beginning (sheath-limited); (ii) quickly grows at higher density (high-recycling); (iii) rapidly drops after reaching the maximum (detachment regime) [73]. However, in the W7-AS and LHD stellarators, the n_{ed} in the divertor shows roughly a linear increase with plasma density at the separatrix [71,74]. No sharp transition from the linear to the high-recycling regime was seen in stellarators. The above difference has been interpreted due to the difference in parallel/perpendicular transport properties between tokamaks and stellarators, in agreement with simulation results by EMC3-EIRENE modeling [75].

At the plasma boundary, the deleterious impurities can be produced through physical sputtering by bombardment of energetic particles (ions and neutrals) onto the target. Thus, lowering energy of the projectiles is essential for reducing the physical sputtering. In this sense, a dense and cold plasma in the divertor region provides favorable environment for reducing the energy of recycling neutrals. The physical mechanisms dominating the edge impurity screening are two forces: one is the friction force between impurities and background ions, which flushes the impurities towards the divertor target (downstream). The other is the ion-temperature gradient force, which drives the impurities towards the plasma core (upstream) [70]. In tokamaks the ion-temperature gradient force is stronger, whereas for stellarators the large cross-field transport in the SOL makes the friction force dominant, and hence, is beneficial for impurity retention in the divertor. Moreover, many more X-points in stellarators can also be helpful to spread the radiation pattern non-uniformly around the entire torus.

7. Quasi-symmetric stellarators

For the optimization of stellarators, an important issue to be considered is to reduce the neoclassical transport. To this end, the quasi-symmetric stellarator has been proposed by several authors [76,77]. In a quasi-symmetric field, the magnetic field should be expressible as a function of the flux surface and a single helicity angle. Within a given flux surface, a guiding center cannot distinguish what field line it is on and the rotational transform is irrational. An example of such a flux surface designed for the quasi-symmetric stellarator (ESTELL [78]) is shown in Fig. 6. For quasi-symmetric stellarators, there are no regimes of $\nu^{0.5}$ and $1/\nu$ transport, and thus, the neoclassical transport is intrinsically ambipolar. The drift-kinetic equation is close to that in tokamaks so that the transport is similar to the lowest order in ρ^* [79]. Nonetheless, one has to bear in mind that it is impossible to achieve exact quasi-symmetry, and a small violation of symmetry can sometimes results in substantially enhanced neoclassical transport [80]. More details on the discussion of a quasi-symmetric stellarator device can be found in Ref. [81].

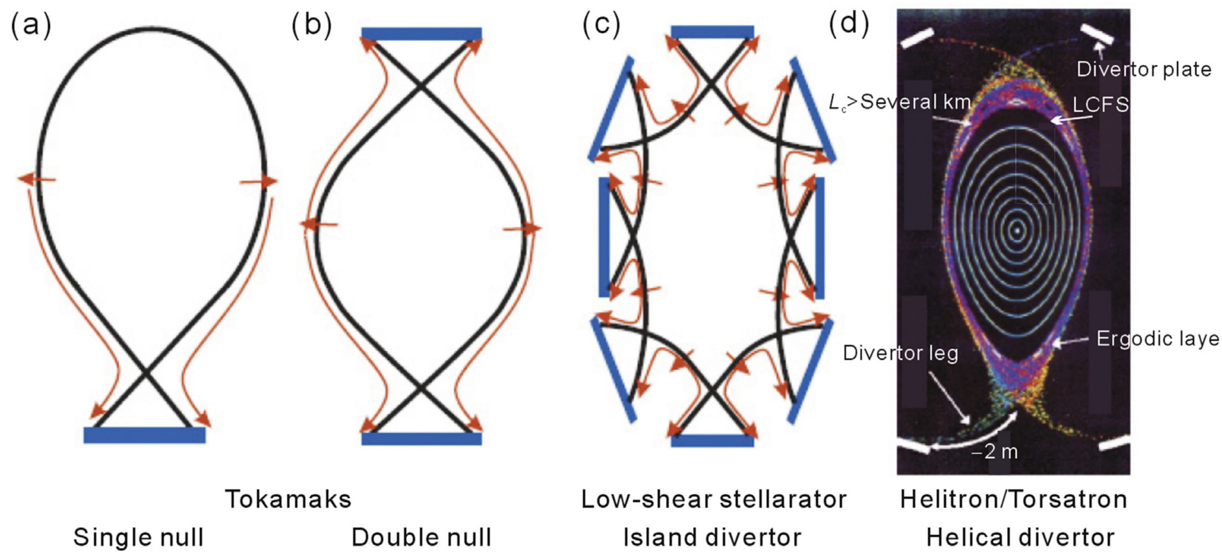

Fig. 5. Schematics of (a) single-null and (b) double-null tokamak divertors; and (c) the intrinsic island divertor for W7-X stellarator and (d) the helical divertor for LHD helitron [70].

8. Future application for fusion reactors

Presently, the extrapolation from the nowadays operating fusion devices to a reactor has been conducted for both tokamak and stellarator configurations. In the direction of the tokamak, ITER (International Thermonuclear Experimental Reactor) is currently under construction in France. It is expected for ITER to generate 500 MW fusion power from ~50 MW input for a period lasting a few minutes (~400 s). But it will only be a scientific demonstration. ITER won't generate electricity. That task will be left for its successor, the prototype power plant DEMO, which will generate several gigawatts of power continuously [1]. On the other hand, various studies of a Helical Advanced Stellarator (HELIAS) have been carried out by extrapolation from the W7-X design [82,83]. With $<\beta> = 4\%-5\%$, the resulting HELIAS reactor concepts have 3 GW of fusion power [84], equivalent to the DEMO design.

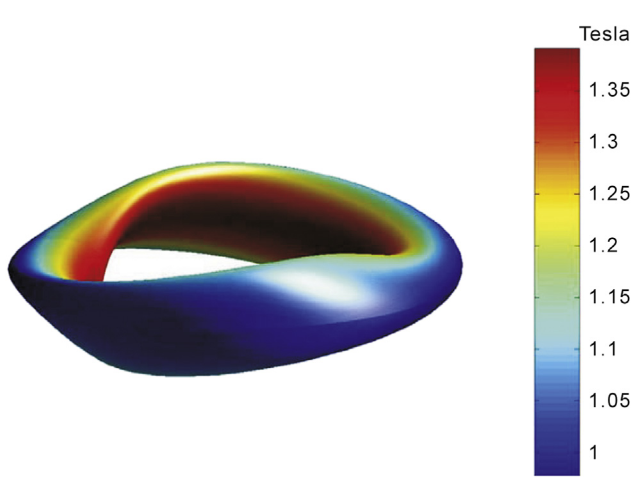

Fig. 6. Schematic of a magnetic flux surface in the quasi-axisymmetric stellarator design ESTELL [78]. The color bar indicates the strength of the magnetic field.

The common problems for DEMO and HELIAS to overcome are heavy heat loads for the divertor, high-energy neutron bombardment for the plasma-facing materials and "tritium breeding blanket", confinement of α-particles with a high pressure gradient in high-Q plasmas and impact of unstable energetic particle modes on plasma performance, *etc.*

In comparison, the main advantages of stellarators are their steady state magnetic field and the absence of current-driven instabilities and disruptions as well as the density-limit issue, whereas for a tokamak reactor the current drive is still lacking a viable solution, as it is not yet clear which method may satisfy. In addition, the relatively large aspect-ratio of stellarators eases the requirements for the blanket design. The disadvantage of stellarators arises from the non-axisymmetric 3-D magnetic field configuration, which results in high level neoclassical transport. In the long mean-free-path regime fast ions in stellarators tend to drift radially and thus leave the confinement region. In order to reduce the neoclassical diffusion and also to well confine fast ions, the effective ripple in stellarators must be kept as small as possible. In this sense, quasi-symmetric or quasi-isodynamic stellarators are optimal choices [84]. Besides, the precision of the fabrication and assembly of coils and coil support structures also complicate the design of stellarator reactors.

9. Summary

In this paper, a general comparison between tokamak and stellarator plasmas was made by reviewing the similarities and differences in their magnetic configuration, MHD behaviors and operational limits, plasmas transport and confinement, plasma rotation and edge/divertor transport. In these two devices, the advantages and disadvantages are as follows: for tokamaks, the advantages include technical simplicity, much lower neoclassical transport (especially at high temperature), stronger toroidal rotations and associated flow-shear, and weaker damping on zonal flows. For stellarators, intrinsically steady-state operation, less MHD activities and nearly disruption-free are great advantages; the stochastic magnetic boundary is also beneficial for impurity retention in the divertor. Turbulence and turbulent transport are comparable in these two systems. Some drift-wave modes are more stable in stellarators. In the energy confinement scaling, an isotope effect appears in tokamaks but not in stellarators. As the number of degrees of the freedom is more for non-axisymmetric systems than axisymmetric ones [85], the possible configurations in stellarators are much more than in tokamaks. For further optimizing stellarator configuration, the quasi-symmetric stellarator has been proposed. If the neoclassical confinement can be substantially improved, the stellarator could be more attractive for a fusion power reactor in the near future.

References

[1] K. Ikeda, Progress in the ITER physics basis, Nucl. Fusion 47 (2007) S1−S404.
[2] V.D. Shafranov, Stellarators, Nucl. Fusion 20 (1980) 1075.
[3] Wendelstein 7-X fusion device produces its first hydrogen plasma, February 03, 2016. http://www.ipp.mpg.de/4010154/02_16.
[4] L. Spitzer, The stellarator concept, Phys. Fluids 1 (1958) 253.
[5] C. Mercier, Equilibrium and stability of a toroidal magnetohydrodynamic system in the neighbourhood of a magnetic axis, Nucl. Fusion 4 (1964) 213.
[6] U. Stroth, A comparative study of transport in stellarators and tokamaks, Plasma Phys. Control. Fusion 40 (1998) 9.
[7] J. Wesson, Tokamaks, fourth ed., Oxford University Press, 2011.
[8] P. Helander, C.D. Beidler, T.M. Bird, M. Drevlak, Y. Feng, et al., Stellarator and tokamak plasmas: a comparison, Plasma Phys. Control. Fusion 54 (2012) 124009.
[9] T. Hayashi, T. Sato, P. Merkel, J. Nührenberg, U. Schwenn, et al., Formation and 'self- healing' of magnetic islands in finite-β helias equilibria, Phys. Plasmas 1 (1994) 3262.
[10] C.C. Hegna, J.D. Callen, Stability of bootstrap current-driven magnetic islands in stellarators, Phys. Plasmas 1 (1994) 3135.
[11] Y. Narushima, K.Y. Watanabe, S. Sakakibara, K. Narihara, I. Yamadaet, et al., Dependence of spontaneous growth and suppression of the magnetic island on beta and collisionality in the LHD, Nucl. Fusion 48 (2008) 075010.
[12] L.C. Bernard, D. Dobrott, F.J. Helton, R.W. Moore, Stabilization of ideal MHD modes, Nucl. Fusion 20 (1980) 1199.
[13] J.W. Connor, J.B. Taylor, Scaling laws for plasma confinement, Nucl. Fusion 17 (1977) 1047.
[14] W.A. Cooper, L. Brocher, J.P. Graves, G.A. Cooper, Y. Narushima, et al., Drift stabilisation of ballooning modes in an inward-shifted LHD configuration, Contrib. Plasma Phys. 50 (2010) 713.
[15] H. Yamada, R. Sakamoto, J. Miyazawa, M. Kobayashi, T. Morisakiet, et al., Characterization and operational regime of high density plasmas with internal diffusion barrier observed in the large helical device, Plasma Phys. Control. Fusion 49 (2007) B487.
[16] G. Waidmann, G. Kuang, Density limits and evolution of disruptions in ohmic TEXTOR plasmas, Nucl. Fusion 32 (1992) 645.
[17] Y. Xu, B.J. Peterson, S. Sudo, T. Tokuzawa, K. Narihara, et al., Properties of thermal decay and radiative collapse of NBI heated plasmas on LHD, Nucl. Fusion 42 (2002) 601.
[18] M. Greenwald, Density limits in toroidal plasmas, Plasma Phys. Control. Fusion 44 (2002) R27.
[19] B. Lipschultz, Review of MARFE phenomena in tokamaks, J. Nucl. Mater. 145−147 (1987) 15.
[20] D.R. Baker, R.T. Snider, M. Nagami, Observation of cold, high-density plasma near the doublet III limiter, Nucl. Fusion 22 (1982) 807.
[21] S. Sudo, Y. Takeiri, H. Zushi, F. Sano, K. Itoh, et al., Scalings of energy confinement and density limit in stellarator/heliotron devices, Nucl. Fusion 30 (1990) 11.
[22] B.J. Peterson, Y. Xu, S. Sudo, T. Tokuzawa, K. Tanaka, et al., Multifaceted asymmetric radiation from the edge-like asymmetric radiative collapse of density limited plasmas in the large helical device, Phys. Plasmas 8 (2001) 3861.
[23] H. Yamada, K. Kawahata, T. Mutoh, N. Ohyabu, Y. Takeiri, et al., Progress in the integrated development of the helical system, Fusion Sci. Technol. 58 (2010) 12.
[24] M. Hirsch, J. Baldzuhn, C. Beidler, R. Brakel, R. Burhenn, et al., Major results from the stellarator Wendelstein 7-AS, Plasma Phys. Control. Fusion 50 (2008) 053001.
[25] Y. Kolesnichenko, A. Könies, V.V. Lutsenko, Y.V. Yakovenko, Affinity and difference between energetic-ion-driven instabilities in 2D and 3D toroidal systems, Plasma Phys. Control. Fusion 53 (2011) 024007.
[26] R. Balescu, Transport Processes in Plasmas: Neoclassical Transport, Elsevier, North Holland, 1998.
[27] F.L. Hinton, R.D. Hazeltine, Theory of plasma transport in toroidal confinement systems, Rev. Mod. Phys. 48 (1976) 239.
[28] S.P. Hirshman, D.J. Sigmar, Neoclassical transport of impurities in tokamak plasmas, Nucl. Fusion 21 (1981) 1079.
[29] L.M. Kovrizhnykh, The energy confinement time in stellarators", Nucl. Fusion 24 (1984) 435.
[30] H.E. Mynick, Transport optimization in stellarators, Phys. Plasmas 13 (2006) 058102.
[31] C.D. Beidler, K. Allmaier, M.Y. Isaev, S.V. Kasilov, W. Kernbichler, et al., Benchmarking of the mono-energetic transport coefficients-results from the International Collaboration on Neoclassical Transport in Stellarators (ICNTS), Nucl. Fusion 51 (2011) 076001.
[32] J.W. Connor, R.J. Hastie, J.B. Taylor, Stability of general plasma equilibria, Plasmas Phys. 22 (1980) 757.
[33] R.L. Dewar, H. Glasser, Ballooning mode spectrum in general toroidal systems, Phys. Fluids 26 (1983) 3038.
[34] J.C. Adam, W.M. Tang, P.H. Rutherford, Destabilization of the trapped-electron mode by magnetic curvature drift resonances, Phys. Fluids 19 (1976) 561.
[35] J.H.E. Proll, P. Helander, J.W. Connor, G.G. Plunk, Resilience of quasi-isodynamic stellarators against trapped-particle instabilities, Phys. Rev. Lett. 108 (2012) 245002.
[36] V. Kornilov, R. Kleiber, R. Hatzky, L. Villard, G. Jost, et al., Gyrokinetic global three-dimensional simulations of linear ion-temperature-gradient modes in Wendelstein 7-X, Phys. Plasmas 11 (2004) 3196.
[37] G. Rewoldt, L.P. Ku, W.M. Tang, Comparison of microinstability properties for stellarator magnetic geometries, Phys. Plasmas 12 (2005) 102512.
[38] P. Xanthopoulos, F. Jenko, Gyrokinetic analysis of linear microinstabilities for the stellarator Wendelstein 7-X, Phys. Plasmas 14 (2007) 042501.
[39] J.A. Baumgaertel, E.A. Belli, W. Dorland, W. Guttenfelder, G.W. Hammett, et al., Simulating gyrokinetic microinstabilities in stellarator geometry with GS2, Phys. Plasmas 18 (2011) 122301.
[40] T.H. Watanabe, H. Sugama, M. Nunami, Effects of equilibrium-scale radial electric fields on zonal flows and turbulence in helical configurations, Nucl. Fusion 51 (2011) 123003.
[41] R.E. Waltz, A.H. Boozer, Local shear in general magnetic stellarator geometry, Phys. Fluids B 5 (1993) 2201.
[42] R. Kleiber, B. Scott, Fluid simulations of edge turbulence for stellarators and axisymmetric configurations, Phys. Plasmas 12 (2005) 102507.
[43] C. Kessel, J. Manickam, G. Rewoldt, W.M. Tang, Improved plasma performance in tokamaks with negative magnetic shear, Phys. Rev. Lett. 72 (1994) 1212.
[44] M. Hugon, B.P.V. Milligen, P. Smeulders, L.C. Appel, D.V. Bartlett, et al., Shear reversal and MHD activity during pellet enhanced performance pulses in JET, Nucl. Fusion 32 (1992) 33.
[45] E.A. Lazarus, L.L. Lao, T.H. Osborne, T.S. Taylor, A.D. Turnbull, et al., An optimization of beta in the DIII-D tokamak, Phys. Fluids B 4 (1992) 3644.

[46] G.T. Hoang, C. Gil, E. Joffrin, D. Moreau, A. Becoulet, et al., Improved confinement in high l_i lower hybrid driven steady state plasmas in TORE SUPRA, Nucl. Fusion 34 (1994) 75.
[47] Y. Kamada, K. Ushigusa, O. Naito, Y. Neyatani, T. Ozeki, et al., Non-inductively current driven H mode with high beta N and high beta p values in JT-60U, Nucl. Fusion 34 (1994) 1605.
[48] W.M. Nevins, et al., Plasma physics and controlled fusion research, in: Proc. 14th Int. Conf vol. 3, IAEA, Vienna, 1992, p. p 279.
[49] C.P. Ritz, et al., Plasma physics and controlled fusion research, in: Proc. 13th Int Conf vol. 2, IAEA, Vienna, 1991, p. p 589.
[50] C. Hidalgo, Edge turbulence and anomalous transport in fusion plasmas, Plasma Phys. Control. Fusion 37 (1995) A53.
[51] M. Endler, H. Niedermeyer, L. Giannone, E. Kolzhauer, A. Rudyj, et al., Measurements and modelling of electrostatic fluctuations in the scrape-off layer of ASDEX, Nucl. Fusion 35 (1995) 1307.
[52] R.J. Fonck, N. Bretz, G. Cosby, R. Durst, E. Mazzucato, et al., Fluctuation measurements in the plasma interior on TFTR, Plasma Phys. Control. Fusion 34 (1992) 1993.
[53] L. Giannone, R. Balbín, H. Niedermeyer, M. Endler, G. Herre, et al., Density, temperature, and potential fluctuation measurements by the swept Langmuir probe technique in Wendelstein 7-AS, Phys. Plasmas 1 (1994) 3614.
[54] X. Garbet, J. Payan, C. Laviron, P. Devynck, S.K. Saha, et al., Turbulence and energy confinement in TORE SUPRA ohmic discharges, Nucl. Fusion 32 (1992) 2147.
[55] S. Sattler, H.J. Hartfuss, Experimental evidence for electron temperature fluctuations in the core plasma of the W7-AS stellarator, Phys. Rev. Lett. 72 (1994) 653.
[56] P.N. Yushmanov, T. Takizuka, K.S. Riedel, O.J.W.F. Kardaun, J.G. Cordey, et al., Scalings for tokamak energy confinement, Nucl. Fusion 30 (1990) 1999.
[57] ITER Physics Expert Group on Confinement and Transport, Chapter 2: plasma confinement and transport, Nucl. Fusion 39 (1999) 2175.
[58] U. Stroth, M. Murakami, R.A. Dory, H. Yamada, S. Okamura, et al., Energy confinement scaling from the international stellarator database, Nucl. Fusion 36 (1996) 1063.
[59] M. Bessenrodt-Weberpals, F. Wagner, O. Gehre, L. Giannone, J.V. Hofmann, et al., The isotope effect in ASDEX, Nucl. Fusion 33 (1993) 1205.
[60] M. Ramisch, N. Mahdizadeh, U. Stroth, F. Greiner, C. Lechte, et al., ρ_s scaling of characteristic turbulent structures in the torsatron TJ-K, Phys. Plasmas 12 (2005) 032504.
[61] B. Liu, M.A. Pedrosa, B.P.V. Milligen, C. Hidalgo, C. Silva, et al., Isotope effect physics, turbulence and long-range correlation studies in the TJ-II stellarator, Nucl. Fusion 55 (2015) 112002.
[62] Y. Xu, C. Hidalgo, I. Shesterikov, A. Kramer-Flecken, S. Zoletnik, et al., Isotope effect and multiscale physics in fusion plasmas, Phys. Rev. Lett. 110 (2013) 265005.
[63] A.D. Gurchenko, E.Z. Gusakov, P. Niskala, A.B. Altukhov, L.A. Esipov, et al., The isotope effect in turbulent transport control by GAMs. Observation and gyrokinetic modeling, Plasma Phys. Control. Fusion 58 (2016) 044002.
[64] T.S. Hahm, L. Wang, W.X. Wang, E.S. Yoon, F.X. Duthoit, et al., Isotopic dependence of residual zonal flows, Nucl. Fusion 53 (2013) 072002.
[65] T.H. Stix, Decay of poloidal rotation in a tokamak plasma, Phys. Fluids 16 (1973) 1260.
[66] V. Rozhansky, M. Tendler, Reviews of Plasma Physics, Plasma Rotation in Tokamaks, 1996. New York-London (Chapter 3).
[67] P. Helander, On rapid plasma rotation, Phys. Plasmas 14 (2007) 104501.
[68] H. Sugama, T.H. Watanabe, M. Nunami, S. Nishimura, Quasisymmetric toroidal plasmas with large mean flows, Phys. Plasmas 18 (2011) 082505.
[69] A. Fujisawa, A review of zonal flow experiments, Nucl. Fusion 49 (2009) 013001.
[70] Y. Feng, M. Kobayashi, T. Lunt, D. Reiter, Comparison between stellarator and tokamak divertor transport, Plasma Phys. Control. Fusion 53 (2011) 024009.
[71] P. Grigull, K. Mccormick, J. Baldzuhn, R. Burhenn, R. Brakel, et al., First island divertor experiments on the W7-AS stellarator, Plasma Phys. Control. Fusion 43 (2001) A175.
[72] N. Ohyabu, T. Watanabe, H. Ji, H. Akao, T. Ono, et al., The large helical device (LHD) helical divertor, Nucl. Fusion 34 (1994) 387.
[73] Y. Shimomura, M. Keilhacker, K. Lackner, H. Murmann, Characteristics of the divertor plasma in neutral-beam-heated ASDEX discharges, Nucl. Fusion 23 (1983) 869.
[74] M. Kobayashi, Y. Feng, S. Masuzaki, M. Shojia, J. Miyazawaa, et al., Divertor transport study in the large helical device, J. Nucl. Mater 363 (2007) 294.
[75] Y. Feng, F. Sardei, P. Grigull, K. Mccormick, J. Kisslinger, et al., Transport in island divertors: 3D modelling and comparison to first experiments on W7-AS, Plasma Phys. Control. Fusion 44 (2002) 611.
[76] J. Nührenberg, R. Zille, Quasi-helically symmetric toroidal stellarators, Phys. Lett. A 129 (1988) 113.
[77] A.H. Boozer, Quasi-helical symmetry in stellarators, Plasma Phys. Control. Fusion 37 (1995) A103.
[78] M. Drevlak, F. Brochard, P. Helander, J. Kisslinger, M. Mikhailov, et al., ESTELL: a quasi-toroidally symmetric stellarator, Contrib. Plasma Phys. 53 (2013) 459.
[79] J.R. Cary, S.G. Shasharina, Omnigenity and quasihelicity in helical plasma confinement systems, Phys. Plasmas 4 (1997) 3323.
[80] S. Gori, W. Lotz, J. Nuhrenberg, Theory Fusion Plasmas (1996) 335.
[81] P. Helander, Theory of plasma confinement in non-axisymmetric magnetic fields, Rep. Prog. Phys. 77 (2014) 087001.
[82] H. Wobig, Theory of advanced stellarators, Plasma Phys. Control. Fusion 41 (1999) A159.
[83] C.D. Beidler, E. Harmeyer, F. Herrnegger, Y. Igitkhanov, A. Kendl, et al., The Helias reactor HSR4/18, Nucl. Fusion 41 (2001) 1759.
[84] R.C. Wolf, C.D. Beidler, R. Burhenn, J. Geiger, M. Hirsch, et al., From Wendelstein 7-X to a Stellarator Reactor, Plasma Fusion Res. 5 (2010) S1011.
[85] A.H. Boozer, Physics of magnetically confined plasmas, Rev. Mod. Phys. 76 (2004) 1071.